Journal of Renewable Materials

Tech Science Press

DOI: 10.32604/jrm.2023.046585

ARTICLE

Novel Sustainable Cellulose Acetate Based Biosensor for Glucose Detection

M. F. Elkady[1,2,*], E. M. El-Sayed[2], Mahmoud Samy[3], Omneya A. Koriem[1] and H. Shokry Hassan[4,5]

[1]Chemical and Petrochemical Engineering Department, Egypt-Japan University of Science and Technology, New Borg El-Arab, Alexandria, Egypt

[2]Fabrication Technology Research Department, Advanced Technology and New Materials Research Institute, City of Scientific Research and Technological Applications (SRTA-City), New Borg El-Arab, Alexandria, 21934, Egypt

[3]Department of Public Works Engineering, Faculty of Engineering, Mansoura University, Mansoura, 35516, Egypt

[4]Environmental Engineering Department, Egypt-Japan University of Science and Technology, New Borg El-Arab, Alexandria, Egypt

[5]Electronic Materials Research Department, Advanced Technology and New Materials Research Institute, City of Scientific Research and Technological Applications (SRTA-City), New Borg El-Arab, Alexandria, 21934, Egypt

[*]Corresponding Author: M. F. Elkady. Email: Marwa.elkady@ejust.edu.eg

Received: 08 October 2023 Accepted: 14 December 2023 Published: 11 March 2024

ABSTRACT

In this study, green zinc oxide (ZnO)/polypyrrole (Ppy)/cellulose acetate (CA) film has been synthesized via solvent casting. This film was used as supporting material for glucose oxidase (GOx) to sensitize a glucose biosensor. ZnO nanoparticles have been prepared via the green route using olive leaves extract as a reductant. ZnO/Ppy nanocomposite has been synthesized by a simple in-situ chemical oxidative polymerization of pyrrole (Py) monomer using ferric chloride ($FeCl_3$) as an oxidizing agent. The produced materials and the composite films were characterized using X-ray diffraction analysis (XRD), scanning electron microscope (SEM), Fourier transform infrared (FTIR) and thermogravimetric analysis (TGA). Glucose oxidase was successfully immobilized on the surface of the prepared film and then ZnO/Ppy/CA/GOx composite was sputtered with platinum electrode for the current determination at different initial concentrations of glucose. Current measurements proved the suitability and the high sensitivity of the constructed biosensor for the detection of glucose levels in different samples. The performance of the prepared biosensor has been assessed by measuring and comparing glucose concentrations up to 800 ppm. The results affirmed the reliability of the developed biosensor towards real samples which suggests the wide-scale application of the proposed biosensor.

KEYWORDS

Biosensors; composite films; glucose; polypyrrole; green ZnO; cellulose acetate

1 Introduction

Diabetes is considered one of the diseases that significantly affects human health, however, statistics show that the number of diabetic patients around the world is consistently increasing. Therefore, measuring and detecting glucose levels plays a vital role in controlling the disease [1,2]. In accordance, developing a sensitive and selective glucose biosensor that converts biological incidents into electrical signals became of great importance [3,4]. Electrochemical biosensors based on enzymes are being widely

used in various analytical applications due to their simplicity, sensitivity, performance, and low cost. Recently, different enzymes namely, glucose oxidase (GOx), urease and cholesterol oxidase are usually used as a catalyst in enzymatic electrochemical biosensors for glucose detection. Amongst the used enzymes, GOx has proved its selectivity for glucose detection besides its low cost represents a promising candidate for biosensor application. The immobilization of GOx on the electrode's surface and detection of the current associated with the enzymatic redox reaction is the major principle of glucose biosensors. Nonetheless, the weak stability of these enzymes on the electrode's surface triggered the researchers to explore numerous support materials such as polymers and nanomaterials [5–9]. As a result, various conducting polymers have been intensively studied for the entrapment of GOx due to their outstanding electroconductive characteristics [10].

Amongst the known conducting polymers, polypyrrole (Ppy) has been frequently used and applied in amperometric biosensors for its good adherence to electrode materials, stability at ambient conditions, and compatibility with different enzymes and preventing them from leaching out [11,12]. Despite the mentioned unique properties of Ppy, its formed films still suffer from some drawbacks such as low mechanical stability and poor processibility which limits its utilization for biomedical applications. Consequently, many attempts have been proposed to overcome those disadvantages including blending with other biopolymers and/or nanoparticle impregnation [10,13,14]. In the last years, nanoparticles, particularly metal oxides have attracted attention for the fabrication of nanocomposites with improved electrocatalytic efficiency and enzymatic immobilization and stability [15,16]. Moreover, they may enhance the electron transport and the sensing properties [17]. The biocompatibility, chemical stability, non-toxicity, high adsorption ability owing to an isoelectric point of 9.5, large surface area, and rapid electron transfer features made zinc oxide (ZnO) a reliable competitive nanomaterial for glucose biosensors [18–20]. ZnO nanoparticles can be synthesized via different chemical techniques, nevertheless, the eco-friendly green synthesis routes using biological materials became more popular as they possess lower toxicity [21,22].

To boost the Ppy's biocompatibility, combining it with other organic materials was the second attempt to be adapted [23]. Cellulose acetate (CA) was found to be applied for bio-sensing applications for its excellent chemical and mechanical stability and biocompatibility. Moreover, cellulose acetate showed unique performance in biomolecule immobilization and biosensing [24–26]. Thus, the preparation of ZnO/Ppy/CA composites is expected to improve the electron migration of the enzymatic reactions, sensitivity, stability and biosensor performance [27].

In the current study, an innovative green biocompatible ZnO/Ppy/CA membrane matrix was fabricated for the immobilization of glucose oxidase for glucose detection biosensors. The characteristics of the fabricated materials have been investigated. The fabrication of glucose biosensors and their measurements have been studied as well. The suitability and sensitivity of the developed biosensor were evaluated by measuring glucose concentration for different samples with known concentrations.

2 Materials and Methods

2.1 Materials

All chemicals were of analytical grade and used as purchased with no additional modifications. Pyrrole (Py) (97%), ferric chloride ($FeCl_3$, 95%), ethanol (C_2H_5OH, 99%) and zinc nitrate ($Zn(NO_3)_2.6H_2O$,98%) were purchased from Sigma Aldrich. Sodium hydroxide (NaOH, 99%), dimethylformamide (DMF, 97%), acetone (95%) and cellulose acetate (CA) (98%) were supplied by Acros organics. Fresh leaves of olive were collected during May from Sohag–Egypt. The leaves were washed thoroughly with tap water followed by distilled water to get rid of any contaminants. Then, they were dried overnight at 70°C and finally grinded to a fine powder. The obtained powder was then stored in an air-tight container until further usage.

2.2 Biosynthesis of Zinc Oxide Nanoparticles

ZnO nanoparticles were fabricated as previously reported in the literature with some modifications [28,29]. The biosynthesis procedures depend on the antioxidants (polyphenols) that were extracted from olive leaves as a reducing agent. First, 15 g of the dried leaves were mixed with 200 ml of distilled water and heated for 2 h at 70°C. The light-yellow extract was then cooled to room temperature, filtered, and stored in the refrigerator. This extract was utilized for the reduction of zinc ions (Zn^{2+}) to (ZnO). Secondly, 70 ml of the metal precursor ($Zn(NO_3)_2.6H_2O$) with a concentration of 0.2 M was reduced using 30 ml of Olive leaf extract. The extract was added dropwise under constant stirring and heating at 60°C for 1 h. The produced powder was stirred overnight to ensure the complete conversion of zinc hydroxide into zinc oxide. The obtained yellowish paste was calcinated at 500°C for 2 h. The white powder was grinded after calcination to produce fine ZnO powder.

2.3 Preparation of ZnO/Ppy Nanocomposites

ZnO/Ppy nanocomposite has been synthesized by a simple *in-situ* chemical oxidative polymerization of Py monomer using $FeCl_3$ as an oxidizing agent. During the synthesis, a certain amount of nano-ZnO was ultrasonicated with a certain amount of water for an hour to obtain a homogeneous dispersion. then, both 0.8 mL of Py monomer and 0.6 g of $FeCl_3$ were added to the mixture and continuously stirred for 4 h at room temperature. The obtained product was then separated and washed with deionized water and ethanol. Afterward, it was dried at 60°C in an oven for 8 h.

2.4 ZnO/Ppy/CA Membrane Preparation

Membranes were prepared by solvent casting technique on a polytetrafluoroethylene (PTFE) dish. Cellulose acetate polymer powder was dissolved in acetone (15 wt% concentration) and stirred for 1 h until a complete homogeneous polymeric solution was obtained. After that, the prepared ZnO/Ppy composite was added with a concentration of (5%). The mixture was mixed using a magnetic stirring device for 24 h and continued with 15 min sonication. Then, the solution was poured into the PTFE dish and kept at room temperature for 24 h to evaporate the solvent.

2.5 Fabrication of Glucose Biosensors

The prepared ZnO/Ppy/CA films have been cut into small pieces (2 cm × 2 cm). Then, these cuts were immersed in a mixture of 5 mL glucose oxidase and phosphate buffer solutions for 24 h to immobilize GOx onto the ZnO/Ppy/CA membrane matrix. After that, the membrane's small pieces were dried at room temperature for 2 h and stored in a refrigerator. Subsequently, platinum (Pt) electrodes were deposited with a thick platinum layer by a plasma sputtering machine as follows: a thin layer of the copper mask was fixed on the top of the sample and the evaporating process occurred to deposit a thin layer of platinum electrodes by a sputtering instrument (Model Hummer 8.1.Turbo Sputtering RF and DC) at a power of 100 W and deposition time of 5 min. Finally, ZnO/Ppy/CA/GOx/Pt electrode has been employed for the electrochemical detection of glucose.

2.6 Analytical Methods

The diffraction peaks of the synthesized materials were identified using an X-ray diffraction (XRD) (6000, Shimadzu). The morphologies and particle sizes were investigated using scanning electron microscopy (SEM). The chemical composition and functional groups of the synthesized materials were studied using Fourier transform infrared spectroscopy (FTIR) (Shimadzu, FTIR-8400S). The wavenumber was selected in the range of 400 and 4000 cm^{-1}. Cyclic voltammetry (CV) was used to measure the response of the prepared electrode. Thermal gravimetric analysis (TGA Q50) was studied to understand the thermal stability of the fabricated materials over the studied temperature range from 10° to 500°C.

2.7 Glucose Biosensing Measurements

ZnO/polypyrrole/cellulose acetate/GOx composite that has been casted on platinum electrode surface can transfer the electrical signal from the active sites of GOx (flavin adenine dinucleotide (FAD)) to the electrode surface as shown in Eqs. (1)–(3) [30] and then the current values were recorded using potentiostat galvanostat auto lab machine. Current values were recorded in the case of different glucose concentrations ranging from 0 to 800 mg/dL. A calibration curve has been developed between glucose concentration and current to measure the concentration of glucose in any sample via the measured current value. The sensitivity and reliability of glucose biosensors were assessed by measuring the concentration of glucose in the case of different samples with known concentrations such as laboratory-prepared glucose solution (100 mg/dl), serum glucose sample (100 mg/dl), plasma glucose sample (100 mg/dl) and blood glucose sample (200 mg/dl). Glucose concentrations of laboratory, serum, plasma and blood samples were determined using spectrophotometer 5010 and Accu-Check glucose determination machine.

$$Glucose + FAD - GO \rightarrow Gluconolactone + FADH_2 - GOx \quad (1)$$

$$FADH_2 - GOx + O_2 \rightarrow FAD - GOx + H_2O_2 \quad (2)$$

$$H_2O_2 \rightarrow O_2 + 2e^- + 2H^+ \quad (3)$$

3 Results and Discussions

3.1 X-Ray Diffraction of the Synthesized Materials

Fig. 1 shows the XRD patterns of pure green ZnO, ZnO/Ppy nanocomposite and ZnO/Ppy/CA membrane with a scan rate of 2°/min. The XRD patterns of ZnO in Fig. 1 show the distinctive peaks at 2θ of 31.7°, 34.4°, 36.2°, 47.5°, 56.6°, 62.8°, 67.9° and 69.1° are ascribed to the diffraction planes of (100), (002), (101), (102), (110), (103), (112) and (201), respectively of wurtzite hexagonal ZnO (JCPDS CARD No. 36-1451) [31,32]. Moreover, the broad peak in the 2θ region 20°–30° confirmed the existence of amorphous polypyrrole in the composite. X-ray diffraction pattern of ZnO/Ppy/CA membrane shows three sets of diffraction peaks which are imputed to cellulose acetate, nano-ZnO, and polypyrrole as portrayed in Fig. 1. The figure also illustrates new peaks at 13.83° and 16.63° are ascribed to cellulose acetate [33]. Accordingly, it was confirmed that the prepared film was successfully prepared from the ZnO/Ppy nanocomposite incorporated at cellulose acetate polymeric matrix. The main feature of cellulose acetate is it's classified as a bio-polymeric network that hosts two conductive materials ZnO and Ppy which are suitable for sensing applications. Both ZnO and Ppy nano-fillers are characterized by their unique and fascinating properties as both have antimicrobial activities, electronic conductivities and bio-compatibilities besides their facile synthesized techniques. So, the fabricated ZnO/Ppy/CA composite membrane is considered as a biocompatible assembly for biosensor application.

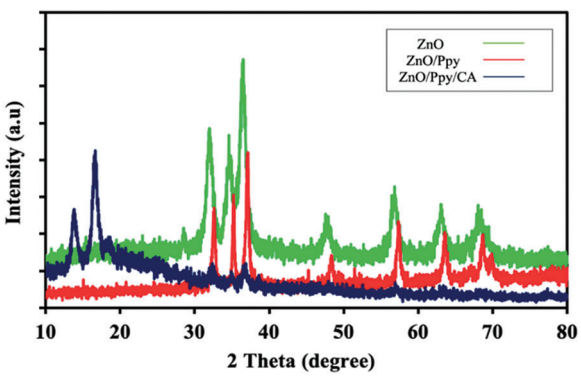

Figure 1: XRD patterns of (a) green synthesized ZnO, (b) ZnO/Ppy composite and (c) ZnO/Ppy/CA film

3.2 Fourier Transform Infrared Spectroscopy (FTIR) of the Prepared Materials

Fig. 2 demonstrates the FTIR spectra of the prepared biosynthesized ZnO, where the peaks at 1639.55, 1635.69, 1456.30 cm^{-1} and all bands at 449.43–557.45 cm^{-1} is attributed to ZnO nanoparticles which correspond to Zn–O stretching and deformation vibration, respectively. The broad peak at 1456.30 cm^{-1} is due to the effect of polyphenols and natural pigments from plant leaf extracts [34]. The broad peaks at 3398.69 and 3439.19 cm^{-1} are due to metal-oxygen (metal oxides) frequencies observed for the respective ZnO nanoparticles. The peaks located at 879 and 900 cm^{-1} are attributed to C–H bonds [35]. Furthermore, the peaks at 1523 and 1543 cm^{-1} correspond to C=C stretching vibration [35]. The peaks at 1660 and 1676 cm^{-1} are ascribed to C=N and C–N bonds, respectively, whereas the peak at 1064 cm^{-1} is attributed to the stretching mode of N–H [36]. The presence of C–C out-of-plane ring deformation vibrations or C–H rocking has been affirmed by the peaks at 677 and 695 cm^{-1} [36]. FTIR spectra showed broad absorption bands at 3400 and 3200 cm^{-1} which are imputed to N–H ring vibrations of polypyrrole [37]. Fig. 2 also displays FTIR spectra of ZnO/Ppy. The bands at 449.43 and 557.45 cm^{-1} are attributed to Zn–O bond stretching and deformation vibration [32]. The same bands in pure polypyrrole were observed in ZnO/Ppy composites with small shifts. For ZnO/Ppy/CA composite, besides the bands of Zn–O bond and pure polypyrrole, the bands at 2947, 1730, 1735 and 1051 cm^{-1} are assigned to CH stretching, C=O stretching, CH_3 stretching and O–CH_3 stretching vibrations of cellulose acetate [38].

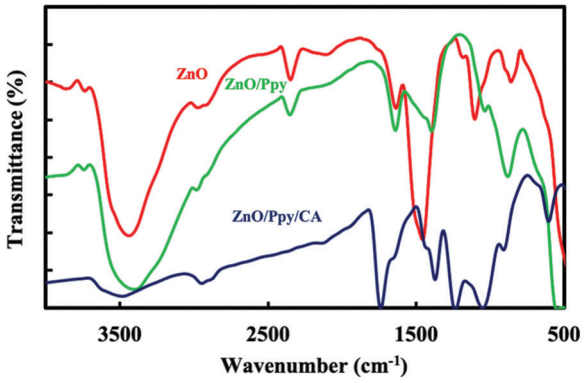

Figure 2: FTIR spectra of (a) green synthesized ZnO, (b) ZnO/Ppy composite and (c) ZnO/Ppy/CA film

3.3 Scanning Electron Microscope (SEM) Analysis

SEM images were used to understand the morphological structure of ZnO, ZnO/Ppy and ZnO/Ppy/CA composite. As can be seen in Fig. 3a, the resulting green nano-ZnO particles are mostly spherical with a particle size ranging from 20 to 80 nm [39]. In addition, SEM images reveal that the prepared ZnO/Ppy composite has different morphologies (e.g., spherical, spongy). As it was presented in Fig. 3b, the Ppy core is covered by ZnO nanoparticles, and this can confirm the formation of ZnO/Ppy nanocomposite [40]. The surface morphology of neat CA and ZnO/Ppy/CA composite are shown in Figs. 3c and 3d, respectively. As shown, neat CA revealed a smooth surface. However, small white particles appeared after the impregnation of ZnO/Ppy composite, which indicates the successful fabrication of ZnO/Ppy/CA membrane. The cross-section images in Figs. 3e and 3f show the formation of a homogeneous sponge-like porous structure membrane with a high degree of porosity.

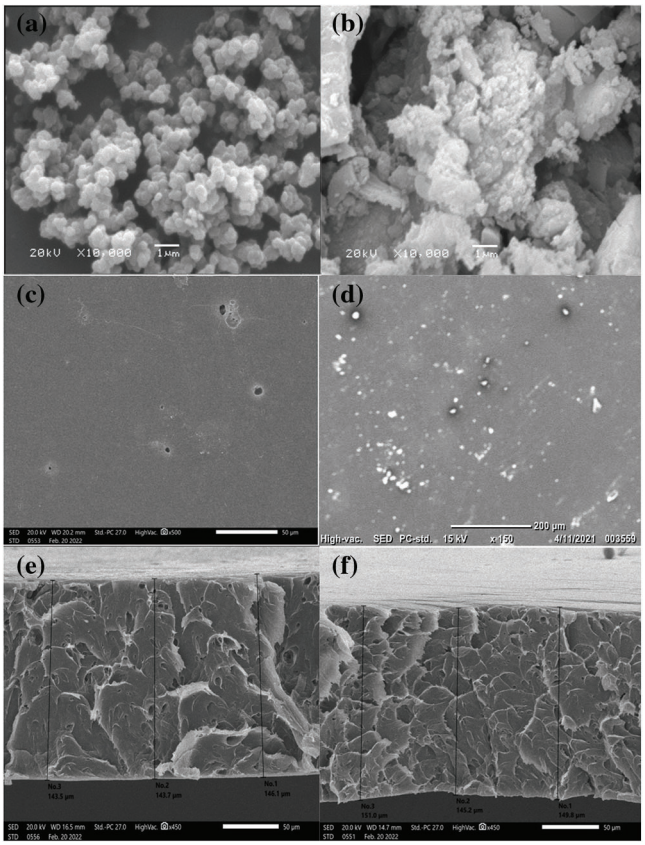

Figure 3: SEM images of (a) Green synthesized nano-ZnO, (b) ZnO/Ppy composite, (c) pure Cellulose acetate film's surface (d) ZnO/Ppy/CA film's surface (e) pure Cellulose acetate film's cross section area and (f) ZnO/Ppy/CA film's cross section area

3.4 Thermal Properties of the Prepared Materials (TGA)

Thermogravimetric analysis (TGA) of the samples was performed under N_2 atmosphere by raising the temperature from room temperature to 500°C. Fig. 4 shows the TGA pattern of the green synthesized ZnO nanoparticles over the studied temperature range. The first degradation step of green synthesized ZnO nanoparticles started at 19°C and ended at around 200°C with a weight loss of almost 2.2% from the original material weight. This could be attributed to the removal of the surface water adsorbed to the green synthesized ZnO nanoparticles. However, the remaining mass of the material remained constant up to 500°C [41,42].

As shown in Fig. 4, the thermal decomposition behavior of ZnO/polypyrrole nanoparticles was investigated by increasing the temperature from 26°C to 500°C. The weight loss at temperatures ranging from 38°C to 177°C was attributed to the removal of water molecules adsorbed on zinc oxide/polypyrrole surface. The increase of the temperature from 177°C to around 282°C resulted in an increase in the weight loss due to the condensation dehydration of the hydroxyls [43]. The last thermal degradation step started at 282°C and ended at around 500°C might be due to the decomposition of the residual organics. The average weight loss ratio of ZnO/polypyrrole nanoparticles was about 51.6%.

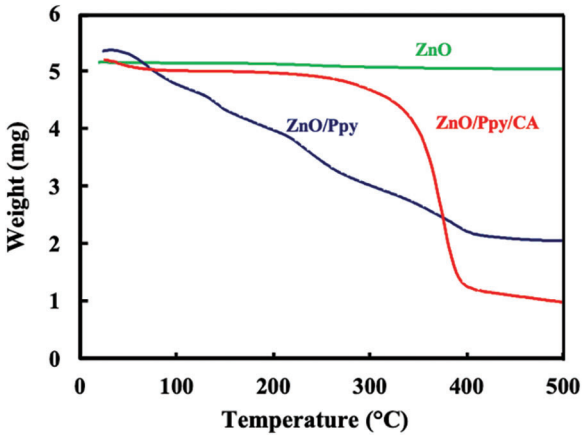

Figure 4: TGA patterns of (a) green synthesized ZnO, (b) ZnO/Ppy composite and (c) ZnO/Ppy/CA film

For the TGA pattern of ZnO/Ppy/CA film. The weight loss was measured by increasing the temperature from 26°C to 500°C. The weight loss at 25°C–210°C was due to the loss of adsorbed water molecules and a weight loss of 2.3% was observed at a temperature range from 210°C to 269°C. A weight loss of 69.5% was observed by raising the temperature from 269°C to 406°C due to the loss of H-bond between cellulose acetate molecules and the loss of O-bond between C–O. Then, a weight loss of 4.58% was attained at temperatures from 406°C to 500°C corresponding to the decomposition of the main chain of the polymeric composite [44]. The ZnO/Ppy/CA membrane showed better thermal stability than the nano-ZnO/Ppy composite.

3.5 Effect of the Electrolyte pH on the Prepared Biosensor Performance

The influence of supporting electrolyte pH solution on the redox behavior of GOx fixed onto the prepared composite electrode has been conducted out by Cyclic voltammetry (CV) in 0.01 M phosphate-buffered saline (PBS) solution with different pH values containing 4 mM glucose at a scan rate of 50 mV/s, as shown in Fig. 5. Two solutions of 0.5 M HCl and 0.5 M NaOH have been used to regulate the pH value of PBS before adding 4 mM glucose solution. Enzymatic performance is largely pH-dependent because the enzymes are stable between the pH of 3.5 and 8.0 and lose their activity at a pH value higher than 8 and lower than 2. As demonstrated in Fig. 5, the electrocatalytic activity was increased from a pH of 5 to a pH of 8 and peaked at approximately a pH of 7. In the present work, the catalytic activity of GOx decreased at pH > 7 because of the irreversible denaturation of the enzyme [45].

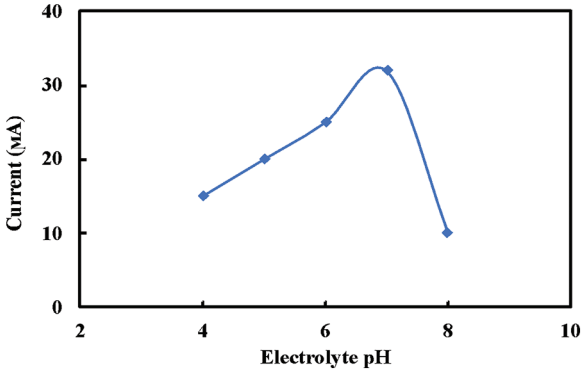

Figure 5: Effect of the electrolyte pH on the prepared electrode response to 4 mM glucose solution

3.6 Evaluation of the Developed Biosensor

Fig. 6 illustrates the dependent relation between the current and a wide range of glucose concentrations. As can be seen, the current increases with increasing glucose concentration due to the rise of H_2O_2 released and consequently more electrical signals are transferred to the electrode [46]. In addition, the figure demonstrates a linear relation with R^2 of 0.965 up to a 500 mg/L glucose concentration. Moreover, the increase in glucose concentration from 500 to 800 mg/L showed a linear plot with R^2 value of 0.938. The linearity of the relation between glucose concentration and current affirmed the suitability and high sensitivity of the constructed biosensor. The unknown glucose concentrations of different samples can be estimated via the linear relationship between current and glucose levels. To evaluate the performance of the prepared biosensor, different glucose samples with known concentrations such as laboratory-prepared glucose solution (100 mg/dl), serum glucose sample (100 mg/dl), plasma glucose sample (100 mg/dl) and blood glucose sample (200 mg/dl) were re-estimated via the current values. The measured glucose concentrations of the different tested samples were approximately the same as their actual concentrations affirming the high sensitivity and accuracy of the developed biosensor.

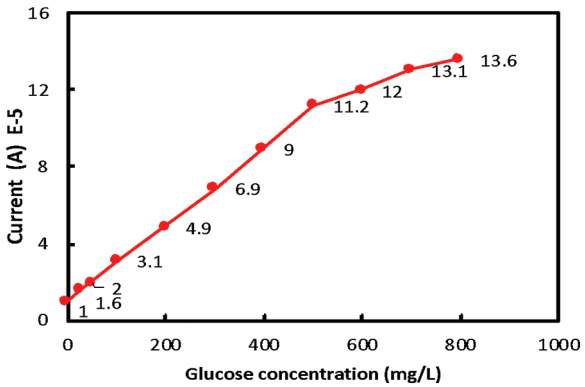

Figure 6: The relation between current and glucose concentration for glucose biosensor

The optimal performance of the electrodes within a sensor requires the choice of suitable materials for the kind of enzymatic reaction taking place. Moreover, the sensor sensitivity can be enhanced by improving the electrode surface area. So, the fabricated ZnO/Ppy/CA/GOx Porous film electrode leads to higher sensitivity due to its large surface area suitable to accommodate the chemical reaction. Moreover, the other key factor to evaluate the quality of the fabricated electrode for measuring glucose concentration is the degree of enzyme immobilization onto the electrode. The permanent immobilization of enzymes grants the reliability of the biosensor for long-term performance. There are various techniques utilized for GOx enzyme immobilization including cross-linked with hydrogel (e.g., chitosan and gelatin), nanomaterials (e.g., carbon nanotubes and graphene) and other stabilizers (e.g., bovine serum albumin) by chemical and physical bonds. The immobilization technique of the fabricated ZnO/Ppy/CA/GOx film electrode was compared with the various immobilization techniques and the materials used in the literature [47,48] for the fabrication of GOx enzyme electrodes for fabrication glucose biosensor in Table 1.

Table 1: Comparable investigation of various GOx enzyme immobilization techniques for fabrication glucose biosensor

Substrate	Immobilization technique
Au/Ag-NCs	Trapping
ITO/Chitosan-Polypyrrole Au-NPs	Trapping
Si/vertically aligned carbon nanofiber	Absorption
Boron-doped diamond/Graphene/Pt-NPs	Absorption
ZnO/Ppy/CA/GOx/Pt (this study)	Absorption
Graphite NPs	Covalent bond

4 Conclusions

Green ZnO nanoparticles, ZnO/Ppy composite and ZnO/Ppy/CA membrane have been synthesized. Various characterization techniques such as XRD, FTIR, SEM and TGA were involved to confirm the chemical structure and the cohesion between the prepared materials and in return the successful fabrication of the composites. Glucose oxidase was successfully supported on ZnO/Ppy/CA membrane and then the immobilized glucose oxidase was coated on the platinum electrode surface for the detection of glucose. The current was measured at different concentrations of glucose and the dependent linear relation between glucose concentration and current affirmed the high sensitivity of the constructed biosensor. The fabricated biosensor has shown high reliability in glucose detection for glucose existing in different samples such as serum, plasma and blood.

Acknowledgement: This work was supported by the Academy of Scientific Research and Technology (ASRT), Egypt (Grant entitled: Manufacturing of Antimicrobial Eco-Friendly Air Filters Integrated with the Air Conditioning Units).

Funding Statement: Not applicable.

Author Contributions: The authors confirm contribution to the paper as follows: study conception and design: E.M.E., M.S., M.E., O.K. and H.S.; data collection: M.E. and H.S.; analysis and interpretation of results: M.S., A.M.H. and M.E.; draft manuscript preparation: E.M.E., M.S., M.E., O.K. and H.S. All authors reviewed the results and approved the final version of the manuscript.

Availability of Data and Materials: Not applicable.

Conflicts of Interest: The authors declare that they have no conflicts of interest to report regarding the present study.

References

1. Liu, Y., Yang, L., Cui, Y. (2023). Transdermal amperometric biosensors for continuous glucose monitoring in diabetes. *Talanta, 253,* 124033.
2. Wang, T. T., Huang, X. F., Huang, H., Luo, P., Qing, L. S. (2022). Nanomaterial-based optical- and electrochemical-biosensors for urine glucose detection: A comprehensive review. *Advanced Sensor and Energy Materials, 1,* 100016. https://doi.org/10.1016/j.asems.2022.100016
3. Mohammadpour-Haratbar, A., Mohammadpour-Haratbar, S., Zare, Y., Rhee, K. Y., Park, S. J. (2022). A review on non-enzymatic electrochemical biosensors of glucose using carbon nanofiber nanocomposites. *Biosensors, 12,* 1004.

4. Cho, I. H., Kim, D. H., Park, S. (2020). Electrochemical biosensors: Perspective on functional nanomaterials for on-site analysis. *Biomaterials Research, 24(1),* 1–12.
5. Sabu, C., Henna, T. K., Raphey, VR., Nivitha, K. P., Pramod, K. (2019). Advanced biosensors for glucose and insulin. *Biosensors and Bioelectronics, 141,* 111201.
6. Arakawa, T., Dao, D. V., Mitsubayashi, K. (2022). Biosensors and chemical sensors for healthcare monitoring: A review. *IEEJ Transactions on Electrical and Electronic Engineering, 17,* 626–636.
7. Bi, R., Ma, X., Miao, K., Ma, P., Wang, Q. (2023). Enzymatic biosensor based on dendritic gold nanostructure and enzyme precipitation coating for glucose sensing and detection. *Enzyme and Microbial Technology, 162*, 110132. https://doi.org/10.1016/j.enzmictec.2022.110132
8. Wang, G., Jiang, G., Zhu, Y., Cheng, W., Cao, K. et al. (2022). Developing cellulosic functional materials from multi-scale strategy and applications in flexible bioelectronic devices. *Carbohydrate Polymers, 283,* 119160. https://doi.org/10.1016/j.carbpol.2022.119160
9. Nemiwal, M., Zhang, T. C., Kumar, D. (2022). Enzyme immobilized nanomaterials as electrochemical biosensors for detection of biomolecules. *Enzyme and Microbial Technology, 156,* 110006.
10. Ebrahimiasl, S., Zakaria, A., Kassim, A., Basri, S. N. (2015). Novel conductive polypyrrole/zinc oxide/chitosan bionanocomposite: Synthesis, characterization, antioxidant, and antibacterial activities. *International Journal of Nanomedicine, 10,* 217–227. https://doi.org/10.2147/IJN.S69740
11. Jiang, G., Wang, G., Zhu, Y., Cheng, W., Cao, K. et al. (2022). A scalable bacterial cellulose ionogel for multisensory electronic skin. *Research, 2022*, 9814767. https://doi.org/10.34133/2022/9814767
12. Raicopol, M., Prună, A., Damian, C., Pilan, L. (2013). Functionalized single-walled carbon nanotubes/polypyrrole composites for amperometric glucose biosensors. *Nanoscale Research Letters, 8,* 1–8. https://doi.org/10.1186/1556-276X-8-316
13. Press, D. (2015). Novel conductive polypyrrole/zinc oxide/chitosan bionanocomposite: Synthesis, characterization, antioxidant, and antibacterial activities. *International Journal of Nanomedicine, 10,* 217–227.
14. Antony, N., Mohanty, S., Nayak, S. K. (2020). Electrochemical inspection of polypyrrole/chitosan/zinc oxide hybrid composites. *Journal of Applied Polymer Science, 137(47),* 49561. https://doi.org/10.1002/app.49561
15. Jain, R., Jadon, N., Pawaiya, A. (2017). Polypyrrole based next generation electrochemical sensors and biosensors: A review. *TrACTrends in Analytical Chemistry, 97,* 363–373.
16. Dakshayini, B. S., Reddy, K. R., Mishra, A., Shetti, N. P., Malode, S. J. et al. (2019). Role of conducting polymer and metal oxide-based hybrids for applications in ampereometric sensors and biosensors. *Microchemical Journal, 147,* 7–24.
17. Kumar, A., Gupta, G. H., Singh, G., More, N., Keerthana, M. et al. (2023). Ultrahigh sensitive graphene oxide/conducting polymer composite based biosensor for cholesterol and bilirubin detection. *Biosensors and Bioelectronics: X, 13,* 100290. https://doi.org/10.1016/j.biosx.2022.100290
18. Elkady, M. F., Shokry Hassan, H., Salama, E. (2016). Sorption profile of phosphorus ions onto ZnO nanorods synthesized via sonic technique. *Journal of Engineering, 2016,* 2308560. https://doi.org/10.1155/2016/2308560
19. Napi, M. L. M., Sultan, S. M., Ismail, R., How, K. W., Ahmad, M. K. (2019). Electrochemical-based biosensors on different zinc oxide nanostructures: A review. *Materials, 12(18),* 2985.
20. Tripathy, N., Kim, D. H. (2018). Metal oxide modified ZnO nanomaterials for biosensor applications. *Nano Convergence, 5,* 1–10.
21. Hassan, H. S., Kashyout, A. B., Morsi, I., Nasser, A. A. A., Raafat, A. (2014). Fabrication and characterization of gas sensor micro-arrays. *Sensing and Bio-Sensing Research, 1,* 34–40. https://doi.org/10.1016/j.sbsr.2014.04.001
22. Diab, K. E., Salama, E., Hassan, H. S., Abd El-moneim, A., Elkady, M. F. (2021). Biocompatible MIP-202 Zr-MOF tunable sorbent for cost-effective decontamination of anionic and cationic pollutants from waste solutions. *Scientific Reports, 11,* 6619. https://doi.org/10.1038/s41598-021-86140-2
23. Zare, E. N., Agarwal, T., Zarepour, A., Pinelli, F., Zarrabi, A. (2021). Electroconductive multi-functional polypyrrole composites for biomedical applications. *Applied Materials Today, 24,* 101117.

24. Yezer, I., Demirkol, D. O. (2020). Cellulose acetate-chitosan based electrospun nanofibers for bio-functionalized surface design in biosensing. *Cellulose, 27,* 10183–10197. https://doi.org/10.1007/s10570-020-03486-y
25. Diagnosis, M. (2020). Recent advances in cellulose-based biosensors for. *Biosensors Review, 10,* 1–26.
26. Buchori, L. (2010). The influence of casting machine speed in cellulose acetate membrane preparation. *International Journal of Science and Engineering, 1(2),* 38–40.
27. Suo, L., Shang, X., Tang, R., Zhou, Y. (2015). The preparation of polypyrrole/cellulose acetate composite films and their electrical properties. *International Conference on Electromechanical Control Technology and Transportation (ICECTT 2015)*, pp. 566–569. Atlantis Press. https://doi.org/10.2991/icectt-15.2015.108
28. Kebede Urge, S., Tiruneh Dibaba, S., Belay Gemta, A. (2023). Green synthesis method of ZnO nanoparticles using extracts of *Zingiber officinale* and garlic bulb (*Allium sativum*) and their synergetic effect for antibacterial activities. *Journal of Nanomaterials, 2023,* 7036247. https://doi.org/10.1155/2023/7036247
29. Ahmed, S., Annu, Chaudhry, S. A., Ikram, S. (2017). A review on biogenic synthesis of ZnO nanoparticles using plant extracts and microbes: A prospect towards green chemistry. *Journal of Photochemistry and Photobiology B: Biology, 166,* 272–284.
30. Yoo, E. H., Lee, S. Y. (2010). Glucose biosensors: An overview of use in clinical practice. *Sensors, 10,* 4558–4576.
31. Kumar, H., Rani, R. (2013). Structural and optical characterization of ZnO nanoparticles synthesized by microemulsion route. *International Letters of Chemistry, Physics and Astronomy, 19,* 26–36. https://doi.org/10.18052/www.scipress.com/ilcpa.19.26
32. Samy, M., Ibrahim, M. G., Gar, M., Fujii, M. (2020). MIL-53(Al)/ZnO coated plates with high photocatalytic activity for extended degradation of trimethoprim via novel photocatalytic reactor. *Separation and Purification Technology, 249,* 117173. https://doi.org/10.1016/j.seppur.2020.117173
33. Omneya, A., Marwa, S., Ahmed, H., Marwa, F. (2023). Cellulose acetate/polyvinylidene fluoride based mixed matrix membranes impregnated with UiO-66 nano-MOF for reverse osmosis desalination. *Cellulose, 30,* 413–426.
34. Faisal, S., Jan, H., Shah, S. A., Shah, S., Khan, A. et al. (2021). Green synthesis of zinc oxide (ZnO) nanoparticles using aqueous fruit extracts of Myristica fragrans: Their characterizations and biological and environmental applications. *ACS Omega, 6(14),* 9607–9722. https://doi.org/10.1021/acsomega.1c00310
35. He, C., Yang, C., Li, Y. (2003). Chemical synthesis of coral-like nanowires and nanowire networks of conducting polypyrrole. *Synthetic Metals, 139(2),* 539–545. https://doi.org/10.1016/S0379-6779(03)00360-6
36. Ruhi, G., Bhandari, H., Dhawan, S. K. (2014). Designing of corrosion resistant epoxy coatings embedded with polypyrrole/SiO_2 composite. *Progress in Organic Coatings, 77,* 1484–1498. https://doi.org/10.1016/j.porgcoat.2014.04.013
37. Fu, Y., Manthiram, A. (2012). Core-shell structured sulfur-polypyrrole composite cathodes for lithium-sulfur batteries. *RSC Advances, 2,* 5927–5929. https://doi.org/10.1039/c2ra20393f
38. Sudiarti, T., Wahyuningrum, D., Bundjali, B., Made Arcana, I. (2017). Mechanical strength and ionic conductivity of polymer electrolyte membranes prepared from cellulose acetate-lithium perchlorate. *IOP Conference Series: Materials Science and Engineering, 223(1),* 12052. https://doi.org/10.1088/1757-899X/223/1/012052
39. Abdelkhalek, A., Al-Askar, A. A. (2020). Green synthesized ZnO nanoparticles mediated by *Mentha spicata* extract induce plant systemic resistance against Tobacco mosaic virus. *Applied Sciences, 10(15),* 5054. https://doi.org/10.3390/app10155054
40. Prakash, S., Rajesh, S., Singh, S. R., Karunakaran, C., Vasu, V. (2012). Electrochemical incorporation of hemin in a ZnO-PPy nanocomposite on a Pt electrode as NO_x sensor. *Analyst, 137,* 5874–5880. https://doi.org/10.1039/c2an36347j
41. Masud, R. A., Islam, M. S., Haque, P., Khan, M. N. I., Shahruzzaman, M. et al. (2020). Preparation of novel chitosan/poly (ethylene glycol)/ZnO bionanocomposite for wound healing application: Effect of gentamicin loading. *Materialia, 12,* 100785. https://doi.org/10.1016/j.mtla.2020.100785
42. Avinash Chunduri, L. A., Kurdekar, A., Eswarappa Pradeep, B., Kumar Haleyurgirisetty, M., Hewlett, I. K. (2017). Streptavidin conjugated ZnO nanoparticles for early detection of HIV infection. *Advanced Materials Letters, 8(4),* 472–480. https://doi.org/10.5185/amlett.2017.6579

43. Escalante, J., Chen, W. H., Tabatabaei, M., Hoang, A. T., Kwon, E. E. et al. (2022). Pyrolysis of lignocellulosic, algal, plastic, and other biomass wastes for biofuel production and circular bioeconomy: A review of thermogravimetric analysis (TGA) approach. *Renewable and Sustainable Energy Reviews, 169,* 112914. https://doi.org/10.1016/j.rser.2022.112914
44. Elkady, M. F., Hassan, H. S. (2021). Photocatalytic degradation of malachite green dye from aqueous solution using environmentally compatible Ag/ZnO polymeric nanofibers. *Polymers, 13(13),* 2033. https://doi.org/10.3390/polym13132033
45. Wang, K., Gu, X., Zhao, Q., Shao, X., Xiao, Y. et al. (2022). H_2O_2/Glucose sensor based on a pyrroloquinoline skeleton-containing molecule modified gold cavity array electrode. *Nanomaterials, 12(10),* 1770. https://doi.org/10.3390/nano12101770
46. Liu, Y., Nan, X., Shi, W. (2019). A glucose biosensor based on the immobilization of glucose oxidase and Au nanocomposites with polynorepinephrine. *RSC Advances, 9,* 16439–16446. https://doi.org/10.1039/c9ra02054c
47. Dong, Z., Yan, L., Qiang, Z., Yixia, Z., Wendong, Z. et al. (2019). Surface stress-based biosensor with stable conductive AuNPs network for biomolecules detection. *Applied Surface Science, 491,* 443–450. https://doi.org/10.1016/j.apsusc.2019.06.178
48. Sang, S., Ge, Y., Ji, J., Yuan, Z., Zhou, C. et al. (2023). Magneto-stress-electric-coupled biosensors originated in magnetostrictive effect for sensitization. *Sensors and Actuators B: Chemical, 378,* 133209. https://doi.org/10.1016/j.snb.2022.133209